Electronic Supplementary Material (ESI) for RSC Advances.

Electronic Supplementary Information

Functionalization of Fullerene at Room Temperature; Toward New Carbon Vectors with Improved Physicochemical Properties

Z. Beiranvand[a], A. Kakanejadifard[a], I. S. Donskyi[b,c], A. Faghani[b], Z. Tu[b], A. Lippitz[c], P. Sasanpour[d,e], F. Maschietto[b], B. Paulus[b], W. E. S Unger[c], R. Haag[b], M. Adeli*[ab]

[a] *Faculty of Science, Department of Chemistry, Lorestan University, Khorramabad, Iran*
[b] *Institut für Chemie und Biochemie, Freie Universität Berlin, Takustrasse 3, Berlin 14195, Germany*
[c]*BAM – Federal Institute for Material Science and Testing, Division of Surface Analysis and Interfacial Chemistry, Unter den Eichen 44-46, 12205 Berlin, Germany*
[d] *Department of Medical Physics and Biomedical Engineering, School of Medicine, Shahid Beheshti University of Medical Sciences, Tehran, Iran.*
[e] *School of Nanoscience, Institute for Research in Fundamental Sciences (IPM), Tehran, Iran*

Contents

Experimental

Materials and methods

All solvents and reagents were purchased from commercial sources (Merck, Sigma Aldrich, and Fluka) and were used directly without further purification.

The human lung carcinoma epithelial cell line (A549) was supplied from DSMZ No. ACC 107. Dulbecco's Modified Eagle Medium (DMEM, low glucose, GlutaMAX™ Supplement, pyruvate) and penicillin/streptomycin were bought from Gibco BRL, Eggenstein, Germany. Fetal calf serum (FCS) was purchased from Biochrom AG, Berlin, Germany.

IR Spectroscopy: Fourier transform infrared spectroscopy (FT-IR) spectra were recorded using a JASCO spectrometer. Ultraultrasonic bath (Model: SONOREX, RK255 HZ, Made in Germany) was used to disperse materials in solvents.

TGA: TGA measurements were recorded by a STA 409 apparatus (Linseis) at temperatures ranging from 25-800 ˚C with a 10 ˚C/min heating rate under argon gas.

Elemental analysis: Elemental analysis was performed using ELEMENTAR apparatus with three columns and detector for carbon, nitrogen, hydrogen elements.

UV-Vis: UV/Vis-measurements were recorded on a Perkin Elmer Lamda 950 UV/Vis/NIR spectrophotometer in the range of 800-280 nm. Samples were measured in quartz cuvettes with square apertures. Millipore quality water was used in all the measurements.

Fluorescence spectroscopy: Fluorescence measurements were performed on the Jasco FP-6500 fluorometer in the range of 500-800 nm. Milli-Q quality water was used for all the experiments. Measurements were performed in quartz cuvettes with square apertures. The width of the excitation and emission bands varied between 3 and 10 nm and the excitation wavelength varied between 480 to 550 nm. For calculation of quantum yield the wavelength was set between 500 and 900 nm with excitation wavelength at 480 nm.

Laser irradiation: The samples were irradiated with 100 W laser Voltcraft ESP1204 with wavelength of 785 nm. The temperature change was measured by thermo camera.

XPS: Gold substrates for the XPS analysis were cleaned in a piranha solution (1:4) 30% H_2O_2: 98% H_2SO_4 (v/v) during ultrasonication at room temperature for 10 min. Then they were washed with the DI water 5 times and with acetone 2 times. After drying overnight Full-Trz was dissolved in methanol and dropwise evenly distributed over the surface of gold substrates. XPS were recorded on a Kratos Axis Ultra DLD spectrometer equipped with a monochromated Al Kα

X-ray source using an analyzer pass energy of 80 eV for survey spectra and 20 eV for the core level spectra. The electron emission angle was 60° and the source-to-analyzer angle was 60°. The binding energy scale of the instrument was calibrated following a Kratos Analytical procedure which uses ISO 15472 binding energy data. Spectra were recorded by setting the instrument to the hybrid lens mode and the slot mode providing approximately a 300 x 700 μm^2 analysis area using charge neutralization. All XPS spectra were processed with the UNIFIT program (version 2017). A Gaussian/Lorentzian sum function peak shape model GL (30) was used in combination with a Shirley background. If not otherwise denoted the L-G mixing for component peaks in all spectra were constrained to be identical. The FWHM of the high energy Cl 2p doublet were allowed to vary in a window of 1–1.6 times the FWHM of the low energy doublet. Peak fitting of C 1s spectra was performed by approximation of symmetric peak for fullerene C 1s component. After peak fitting of the C 1s spectra, all the spectra were calibrated in reference to the fullerene C 1s component at a binding energy of 284.6 eV. High-resolution core-level spectra were recorded in FAT (fixed analyser transmission) mode at a pass energy of 20 eV for all elements: O 1s, N 1s, C 1s, Cl 2p and S 2p.

NEXAFS: NEXAFS measurements have been carried out at the synchrotron radiation source BESSY II (Berlin, Germany). NEXAFS spectra were acquired at the HESGM monochromator dipole magnet CRG beamline.

NEXAFS spectra were acquired in total electron yield (TEY) mode using a channel plate detector. The resolution $E/\Delta E$ of the monochromator at the carbonyl π^* resonance ($h\nu$= 287.4 eV) was in the order of 2500. Raw spectra were divided by ring current and monochromator transmission, the latter obtained with a freshly sputtered Au sample[1]. Alignment of the energy scale was achieved by using an I_0 feature referenced to a C1s → π^* resonance at 285.4 eV measured with a fresh surface of HOPG (highly ordered pyrolytic graphite, Advanced Ceramic Corp., Cleveland, USA)[2]. All NEXAFS spectra are shown in units of the absorption edge jump after subtraction of the pre-edges followed by normalization of the post-edge count rates to one[1]. Both C K- and N K-edges were measured at 55° incident angle of the linearly polarized synchrotron light beam.

Confocal laser scanning microscopy imaging

Cell culture was performed in accordance with German genetic engineering law and German biosafety guidelines (level 1).

A549 cells were cultured in DMEM with 10% (v/v) FCS and 1% penicillin/streptomycin, and incubated in a humidified atmosphere with 5% CO_2 at 37 °C.

A549 cells were seeded into 8-well plates (3×10^4 cells/well). After incubation for 24 h, the original medium was replaced by Full-Z and Full-Trz-PG solution (30 µg/mL in DMEM). Cells were incubated for the following 4 h before culture medium solutions were removed and the wells were rinsed with PBS twice. Then the cells were observed by CLSM (Leica TCS SP8) after the staining of nucleus with Hoechst for 30 min. The excitation and emission for Hoechst was 350 nm and 460 nm, respectively and the excitation and emission for tested compounds was 488 nm and 540 nm, respectively.

Synthesis of Full-Trz

Sodium azide (1.84 g, 28 mmol) dispersed in N-methyl-2-pyrrolidone (NMP) (10 mL) was added dropwise to a solution of cyanuric chloride (triazine) (5.22 g, 28 mmol) in NMP (20 mL) at 0 °C and stirred for 30 minutes. This mixture was added then to a well sonicated solution of C_{60} (200 mg, 0.28 mmol) in NMP (70 mL) and stirred for further 2 hours at 0 °C. The reaction mixture was allowed to reach to the room temperature and stirred overnight. Reaction flask was sonicatedthe day after several times and stirred for an additional day at 25 °C. Solvent was removed by centrifugation and product was washed with water three times and then dialyzed against water for two days. Then it was lyophilized to obtain a light brown, powder. Yield was 80%.

Synthesis of hyperbranched polyglycerol with 5% amino functional groups hPG-$(NH_2)_{5\%}$

hPG-$(NH_2)_{5\%}$ was synthesized according to reported procedure in literature. In a three-step protocol, hyperbranched polyglycerol (PG, molecular weight of M_n = 7200 $g.mol^{-1}$, PDI < 1.2, and a degree of branching of ~50%) was mesylated and subsequently transformed to azido-functionalized derivative through reaction with sodium azide in aqueous solution. Finally, reduction of azide functional groups to amino analogs using triphenylphosphine resulted in hPG-NH_2[3,4].

Synthesis of Full-Trz-PG

Full-Trz (0.02 g, 1.46×10^{-5} mol) was dispersed in NMP (10 mL) and sonicated at room temperature for 5 minutes. hPG-$(NH_2)_{5\%}$ (M_n = 7200 g.mol^{-1}) (0.25 g) was dissolved in NMP (15 mL) and added to the Full-Trz dispersion at 0°C. Then Et_3N (0.1 mL, 7×10^{-4} mol) was added to the reaction flask and mixture was stirred at this temperature for 2 hours and then at 25°C for 24 hours. The product was dialyzed (MWCO 10 kDa) against water for 3 days and later was dried by lyophilization. Yield of reaction was 70%.

Characterization

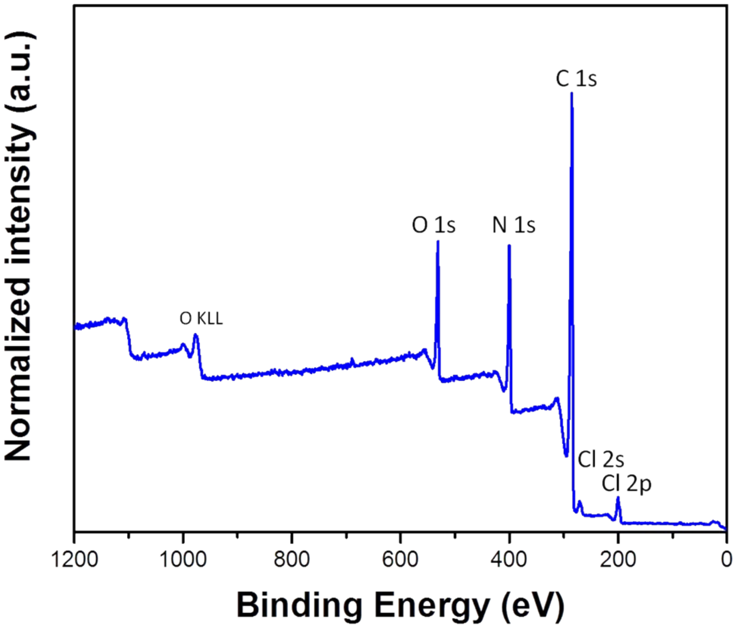

Figure S1. Survey XPS spectrum of Full-Trz showing oxygen, nitrogen, carbon, and chlorine.

Table S1. Interpretation of the fitted components in the highly resolved XPS spectra.

Sample	Spectrum	Binding energy	L-G Mixing	FWHM	Interpretation	Relat. Area	Abs. Area
Full-Trz	C 1s	284.6	0.04	1.59	C-C sp^2	0.38	8624
		286.1	0.04	1.75	C-N, C-Cl, C-O	0.21	4797
		288.0	0.04	1.91	C=O	0.29	6645
		289.9	0.04	1.91	COO, COOH	0.08	1975

		291.6	0.04	1.91	π-π* shake up	0.03	786

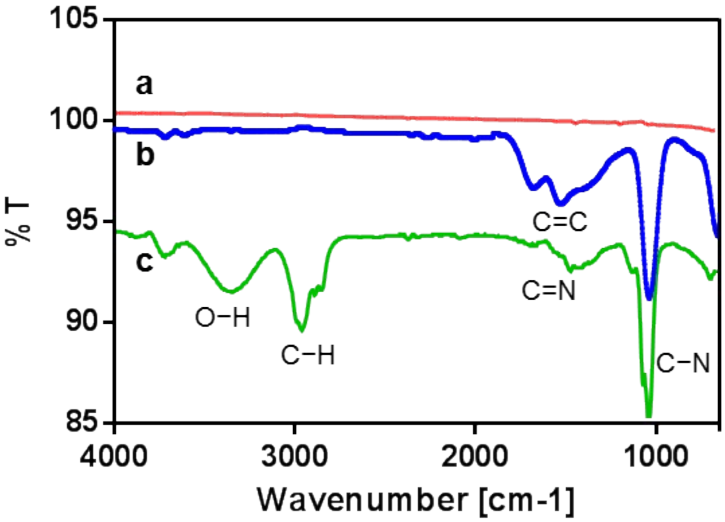

Figure S2. a), b), and c**)** IR spectra of (a) fullerene, (b) Full-Trz, and (c) Full-Trz-PG, respectively.

Figure S2 shows IR spectra of fullerene, Full-Trz and Full-Trz-PG. Absorbance bands at 1510 cm^{-1} and 1634 cm^{-1} are assigned to the C=N and C=C bonds of triazine and the π conjugated system of fullerene, respectively. In the IR spectra of Full-Trz-PG, absorbance bands at 1010 cm^{-1}, and 1065 cm^{-1} are assigned to the C-N and C-O bonds, respectively[5]. Two peaks at the 3365 and 2985 cm^{-1} are corresponded with the O−H and C−H bonds, respectively.

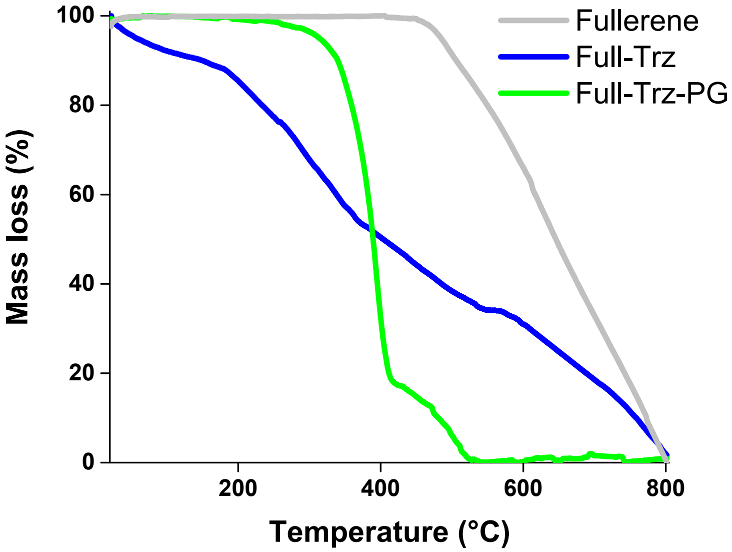

Figure S3. TGA thermograms of fullerene, Full-Trz, and Full-Trz-PG.

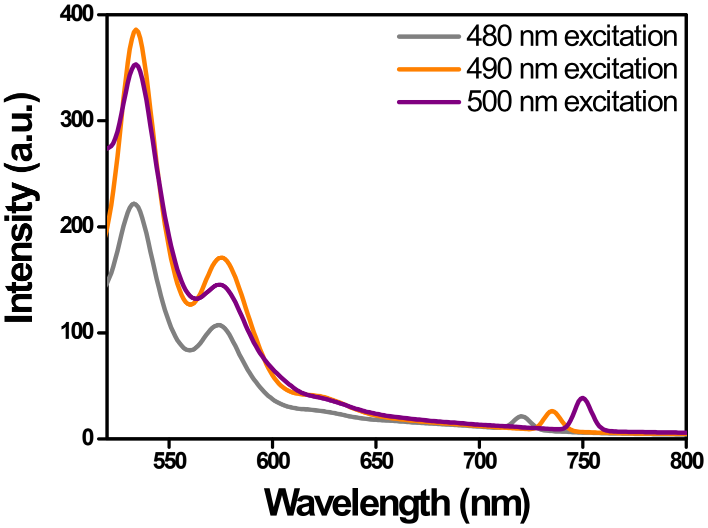

Figure S4. Fluorescence spectra of Full-Trz (0.1 mg/ml) in PBS at different excitation wavelengths.

Excitation at different wavelengths leads to slightly different resulting fluorescence spectra of Full-Trz. These results correlate with broad UV absorbance band of the compound, making it promising candidate for the bioimaging applications at different windows.

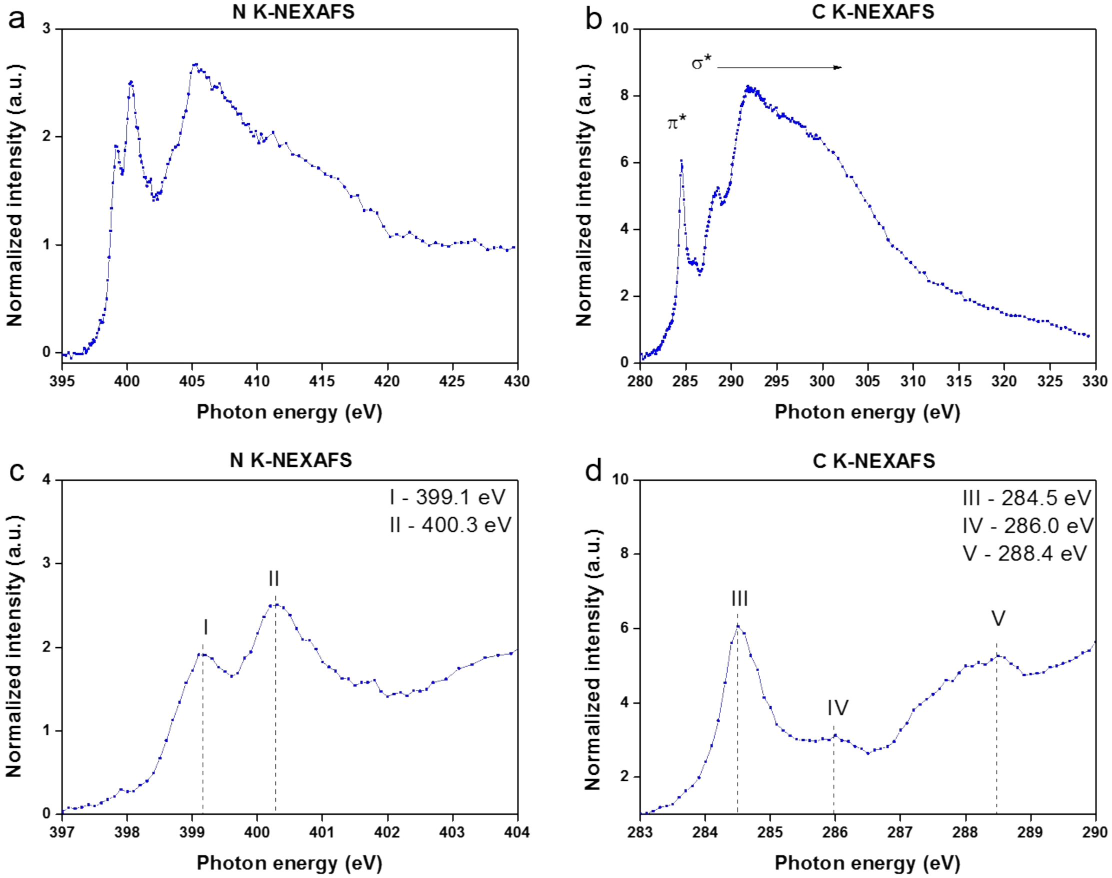

Figure S5. (a) N K-edge NEXAFS, (b) C K-edge NEXAFS; expanded low energy section of (c) N K-edge NEXAFS of Full-Trz and (d) C K-edge NEXAFS.

The C K-edge NEXAFS spectra for Full-Trz is displayed in Fig. S4b,d. At the low-energy side, the NEXAFS spectrum shows a sharp resonance at a photon energy of 284.5 eV (III) corresponding to a C1s → π* transition[6]. This asymmetric peak also corresponds to a ring related C 1s → $\pi^*_{C=N}$ resonance for the conjugated triazine. Literature data of conjugation of triazine to fullerene was not found, but coupling of triazine to graphene showed similar peaks in C K-edge spectra in the range of photon energies 288.1-288.6 eV[7,8], which is near to the resonance V in our experiment.

Table S2. Resonances in the C and N K-edge NEXAFS measured for Full-Trz[6-10].

Sample		Photon energy	Assignment
		N K-edge NEXAFS	
Full-Trz	I[9,10]	399.1	N1s →π* (triazine ring)
	II[7]	400.2	N1s →π* (triazine ring)
		C K-edge NEXAFS	
Full-Trz	III[6]	284.5	C1s →π*
	IV	286.0	C1s →π*, C 1s → $\sigma^*_{C\text{-}N}$, C1s →$\pi^*_{C=N}$
	V[7,8]	287.9-288.5	C1s →π*, C 1s → $\sigma^*_{C\text{-}N}$, C1s →$\pi^*_{C=N}$

Modeling of the UV absorption of fullerene derivatives

In order to calculate the absorption of the structures, as a rough estimation, we have used interaction of light as an electromagnetic wave with the structure. In this regards, 3 different structures are considered as, Fullerene (single sphere), Full-Trz (Spherical Core shell) and Full-Trz-PG (Spherical Core+double shell). The interaction of light with these three spherical structures (Figure S6) has been calculated by solving Maxwell's equations. In this regards, based on spherical structure, Mie theory has been used (expansion of electric and magnetic component of incident and scattered light in spherical Bessel functions)[11]. The dielectric properties of each layer has been exploited based on the experimental measurements[12,13].

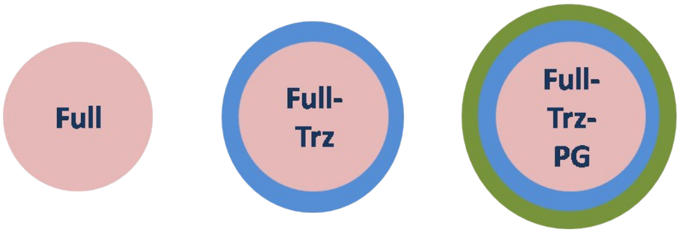

Figure S6. Considered geometry for Mie calculation.

Based on the results of modeling, Figure S7 shows the extinction cross section for 3 different structures. Considering the experiment results for UV-VIS absorption, the calculated results have the same trend. The difference between absorption of different structures, although obtained through classical modeling as a rough estimation, is eloquent of the important effect of surface coating on the absorption properties accordingly.

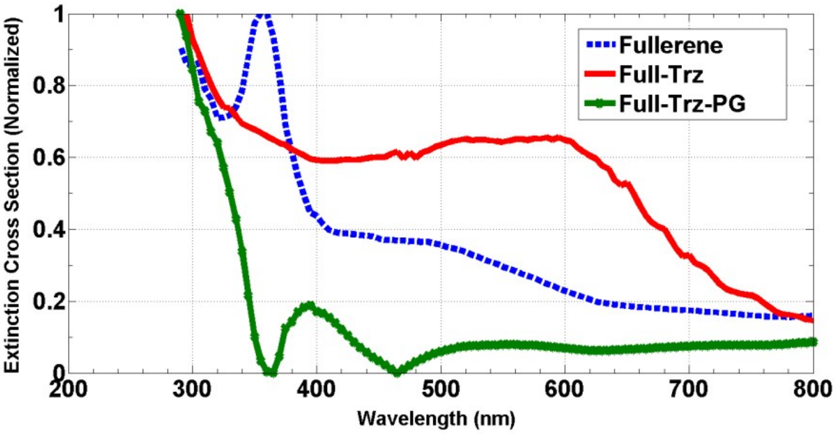

Figure S7. Extinction Cross Section of fullerene, Full-Trz and Full-Trz-PG.

Figure S8. Photograph of PBS solution (1 mg/mL) of Full-Trz-PG (left) and polyglycerol (right).

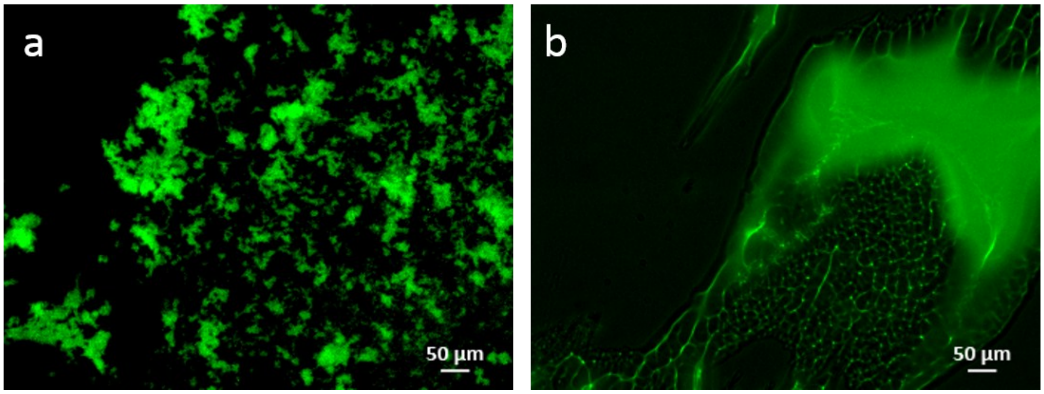

Figure S9. Fluorescence microscopy images of (a) Full-Trz and (b) Full-Trz-PG in the solid state.

Quantum yield was measured using the flowing equation[14]:

$$Q = Q_r \frac{I}{I_r} \frac{OD_r}{OD} \frac{n^2}{n^2{}_r},$$

Where Q – quantum yield, Q_r – reference quantum yield, I – fluorescence intensity integral, I_r – fluorescence intensity integral of the reference compound, OD – value of absorption intensity at 480 nm wavelength of the sample, OD_r – value of absorption intensity at 480 nm wavelength of the reference sample, n – refractive index of the solvent of the sample, n_r – refractive index of the solvent of the reference compound.

Pure fullerene was used as a reference compound for calculation of the quantum yield[15].

Table S3. Energies of the frontier orbitals in eV, along with the HOMO-LUMO gap, for the selected species, calculated at the M06-2X/def2-SVP level of theory.

Sample	HOMO	LUMO	Δ HOMO-LUMO
6,6-Full-Trz	-7.524	-3.206	+4.318
5,6/6-Full-Trz	-7.560	-3.237	+4.323
5,6/5-Full-Trz	-7.658	-3.219	+4.438
Fullerene	-7.556	-3.066	+4.489

Computational details

We have performed DFT calculations for the 2-azido-4,6-dichloro-1,3,5-triazine, pristine fullerene as well as for the fullerene functionalized in different positions. All the calculations were carried out using the Turbomole[16] Program Package for ab initio Electronic Structure Calculations.

The M02-2X[17] hybrid exchange-correlation potential functional was used throughout.

The use of the latter hybrid functional ensures that the HOMO-LUMO gaps, which are usually underestimated by pure DFT methods are corrected by incorporating a percentage of exact Hartree Fock exchange energy (54%) [17].

The split basis set def2-SVP[18], which is the numerical equivalent of the Gaussian 6-31G* basis set, was used for all the calculations. The def2 basis set has been widely used in the theoretical calculations of similar systems, including covalent functionalization of fullerenes.

All systems were geometrically optimized at the M06-2X/def2-SVP level of theory, using the spin-restricted formalism. The convergence thresholds for energy change, maximum displacement and maximum force between optimization cycles were set at 2.0×10^{-8} Hartree, 0.005 Å and 0.004 Hartree*$Å^{-1}$, respectively, so that the optimization procedure was arrested when the energy convergence was satisfied, along with either the displacement or gradient criterion. Frequency calculations indicated that all optimized structures correspond to minima.

The binding energies, calculated as the energy difference between the Full-Trz and the sum of the energies of the isolated species indicated that the [2+1] cycloaddition reaction is thermodynamically favored.

The Nudged Elastic Band (NEB) method supplied with the Climbing Image option (CI-NEB)[19,20] was used to investigate the minimum energy path (MEP) of the [2+1] cycloaddition, starting from two selected stationary configurations. A total of 17 intermediate structures between the endpoints were optimized, allowing for an accurate description of the reaction path.

The NEB method is very efficient in finding the MEP, however the method does not include rigorous convergence to the saddle points, therefore typically none of the images occurs exactly at these locations. The CI-NEB allows to locate the saddle points, and to the optimize the transition states, at the price of a more onerous converge procedure. Therefore a convenient approach is to combine the two methods.

The NEB calculations performed within this work combine the latter two methods.

First a MEP search was performed, using the classical NEB. Second, the climbing image was turned on, in order to optimize the transition state along the previously optimized path. All NEB and CI-NEB calculations have been performed using the ASE package[21].

Computational studies

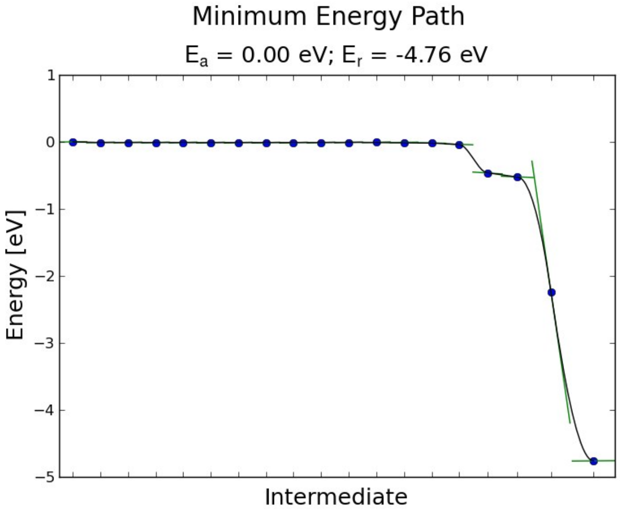

Fig. S10 Minimum energy path for the functionalization reaction of fullerene by in situ [2+1] nitrene cycloaddition at room temperature (Scheme 1), calculated using the CI-NEB[14,15] (Climbing Image Nudged Elastic Band) method. The convergence criterion is set to 0.5 eV/Å. The two fragments (barycenters) are initially separated by ~10 Å.

Table S4. Data for calculations of quantum yields by relative method.

Sample	I	I_r	OD*10^{-3}	OD_r	n	n_r	Q*10^{-4}
Fullerene	1028	1028	8.95	8.95	1.4921	1.4921	2.6
Full-Trz	3451	1028	1.6	8.95	1.4921	1.4921	48.8
Full-Trz-PG	1093	1028	0.8	8.95	1.3325	1.4921	22.9

References

1. J. Stöhr, *Principles, Techniques, and Instrumentation of NEXAFS*, Springer Berlin Heidelberg, Berlin, Heidelberg, 1992.
2. P. E. Batson, *Phys. Rev.,* 1993, *B***48,** 2608-2610.
3. S. Roller, H. Zhou, and R. Haag, *Molec. Divers.,* 2005, **9,** 305-316.
4. P. Ofek, W. Fischer, M. Calderón, R. Haag, and R. Satchi-Fainaro, *FASEB J.* 2010, **24,** 3122-3134.
5. H. L. Spell, *Anal. Chem.* 1967, **39**~~(2)~~, 185-193.
6. R. Mitsumoto, *J. Phys. Chem. A.,* 1998, **102**, 552-560.
7. A. Faghani, I. Donskyi, M. Gholami, W. E. S. Unger, C. Böttcher, J. P. Rabe, R. Haag and M. Adeli, 2016, Submitted.
8. A. Fujimori, N. Sato, K. Kanai, Y. Ouchi and K. Seki, *Langmuir,* 2009, **25,** 1112-1121.
9. E. Apen, A. P. Hitchcock and J. L. Gland, *J. Phys. Chem.,* 1993, **97,** 6859-6866.
10. G. Vall-llosera, B. Gao, A. Kivimaeki, M. Coreno, J. A. Ruiz, M. Simone, H. Agren, and E. Rachlew, *J. Chem. Phys.,* 2008, **128,** 139901.
11. M. Kerker, *The scattering of light, and other electromagnetic radiation*, Academic Press, New York, 1969.
12. R. Belka, *Proceedings of SPIE*, 8903, 2013, 89030B-89030B-8.
13. M. Kelly, P. Etchegoin, , D. Fuchs, W. Krätschmer and K. Fostiropoulos, *Physical Review B,* 1992, **46**, 4963.
14. A. T. R. Williams, S. A. Winfield and J. N. Miller, *Analyst*, 1983, **108**, 1067.
15. B. Ma and Y. P. Sun, *J. Chem. Soc., Perkin Trans. 2,* 1996, **10**, 2157-2162.
16. TURBOMOLE V6.2 2010, a development of University of Karlsruhe and Forschungszentrum Karlsruhe GmbH, 1989-2007, TURBOMOLE GmbH, since 2007; available from http://www.turbomole.com.
17. Y. Zhao and D. G. Truhlar, *Theor. Chem. Account*, 2008, **120**, 215–241.
18. S. Grimme, J. Antony, S. Ehrlich and H. Krieg, *J. Chem. Phys.,* 2010, **132**, 154104-2.
19. D. Sheppard, R. Terrell and G. Henkelman, *J. Chem. Phys*., 2008, **128**, 134106s.
20. G. Henkelman, B. Uberuaga and H. Jónsson, *J. Chem. Phys.* 2000, **113**, 9901-9905.
21. S. R. Bahn, K. W. Jacobsen, *Computing in Science and Engineering*, 2002, **4**, 54-56.